

crystal with the same dimensions was employed. Both crystals were curved cylindrically to a radius of 25.4 cm and viewed the targets through a 0.2-mm wide Ta slit. The energy calibration of the spectrometer was realized by measuring the $K\alpha_{1,2}$ x-ray transitions of Ca, Sc, Ti, V, Cr, Mn, Fe and Co and using as references the energies quoted by Bearden [5]. The $K\alpha_{1,2}$ transitions whose widths were deduced from the values reported in [1] were also employed to determine the instrumental resolution of the spectrometer. The latter was found to vary between 1.45 eV at 3.6 keV and 2.15 eV at 5.9 keV (LiF crystal) and between 1.50 eV at 5.9 keV and 1.55 eV at 6.9 keV (SiO₂ crystal).

The von Hamos spectrometer was installed at the x-ray microscopy beamline ID-21 downstream of the STXM microscope chamber to which it was connected through a 180-cm-long evacuated pipe. On the spectrometer side the pipe was closed with a 25- μ m thick Kapton window to permit an access to the spectrometer chamber without degrading the high-vacuum in the beamline. The x-ray beam was monochromatized with a fixed exit Si (111) double-crystal monochromator with a resolving power of 10^4 . An upper harmonics rejection better than 10^{-3} could be obtained, using Si-based Ni and Si-based Rh coated mirrors for energies below and above 6.5 keV, respectively. Due to the weak intensity of the L_3 - M_1 transitions, 10^{11} - 10^{12} incident photons/s were needed on the targets to obtain data of sufficient statistical quality. For this reason a beam size of 2 mm was employed. For illustration the measured L_3 - M_1 x-ray line of ^{64}Gd is shown in Fig.1.

Eighteen different x-ray beam energies ranging from 4047 eV up to 8086 eV were employed for the photoionization of the targets. As a result of $L_{1,2}L_3N_i$ Coster-Kronig transitions L_3 x-ray lines may be broadened by N satellites that cannot be resolved from the parent diagram lines because the energy shift of the satellites is smaller than the natural width of the transitions. This difficulty was circumvented by irradiating the targets with x-ray beams whose energies were bigger than the L_3 edge but smaller than the L_1 and L_2 edges. The broadening resulting from unresolved N satellites is shown in Fig. 2 where the L_3 - $M_{4,5}$ transitions of Ba excited with synchrotron radiation (no satellite) and bremsstrahlung from an x-ray tube (overlapping N-satellites) are depicted. Similarly, as a result of shake processes, the $K\alpha$ lines of light elements can be markedly broadened by unresolved M satellites. Here again the problem was solved by exciting the calibration targets with photons with energies just above the K-shell ionization threshold.

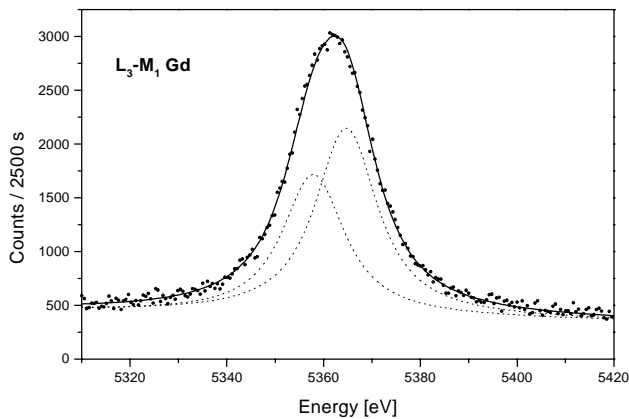


Fig. 1: High-resolution L_3 - M_1 x-ray line of ^{64}Gd . To account for the splitting effect the transition was fitted with two Voigtians having the same width (see text).

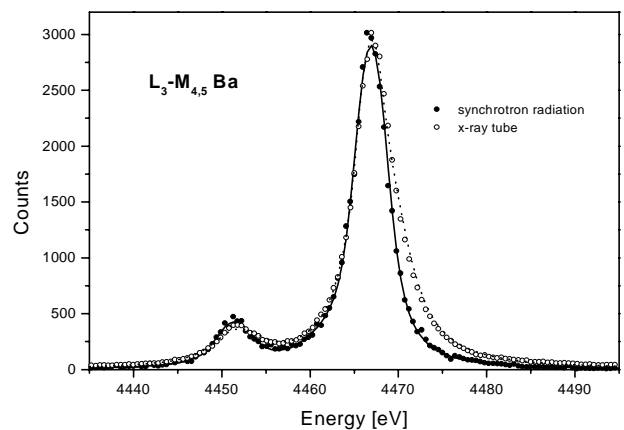


Fig. 2: ^{56}Ba L_3 - $M_{4,5}$ x-ray lines induced by photoionization using 5297 eV synchrotron radiation (L_3 edge at 5247 eV) and bremsstrahlung from a Au x-ray tube operated at 20 kV.

Data analysis and results

The data analysis was performed as follows: the spectra were first corrected to account for the non-uniform beam intensity distribution on the target, using the beam intensity profiles that were measured during the experiment for each beam energy. The corrected spectra were then analysed with a least-squares-fitting code employing Voigtian functions to reproduce the line shape of the transitions. Voigtian profiles were chosen because they correspond to the convolution of the Gaussian instrumental response of the spectrometer with the Lorentzian shape characterizing x-ray transitions. For each transition, the Lorentzian width, centroid energy and intensity as well as a linear background were used as free fitting parameters, whereas the Gaussian

width corresponding to the instrumental broadening was kept fixed at the value determined from the calibration measurements. Finally, as mentioned above, the widths of the atomic-level M_1 were deduced from the widths $\Gamma_{M_{4,5}}$ reported in [1] and the Lorentzian widths of the L_3 - $M_{4,5}$ and L_3 - M_1 transitions obtained from the fits. The M_1 level widths obtained with this method for the rare-earth elements were found to be significantly bigger than the values expected from an interpolation between the lower- Z elements (Xe, Ba, La) and some higher- Z elements (Yb, W, Ir) that were measured with the same spectrometer during another experiment performed at the beam-line BM 5. The deviations between the observed and expected results were found to grow with the total spin S of the open $4f$ subshell, indicating that the splitting effect observed for the $2s$ level does also affect the $3s$ level. As a consequence, the L_3 - M_1 transitions of the rare-earth elements were fitted with two components. The intensity ratios of the two components were determined using the model presented in [3]. For a given element, the width of the two components was kept fixed in the fit at the value expected from the interpolation whereas the energy separation between the two lines was let free. An example of 2-component fit is shown for Gd in Fig. 1. For lanthanides, the M_1 level widths were determined from the FWHM width of the profile obtained by summing the two fitted Lorentzians.

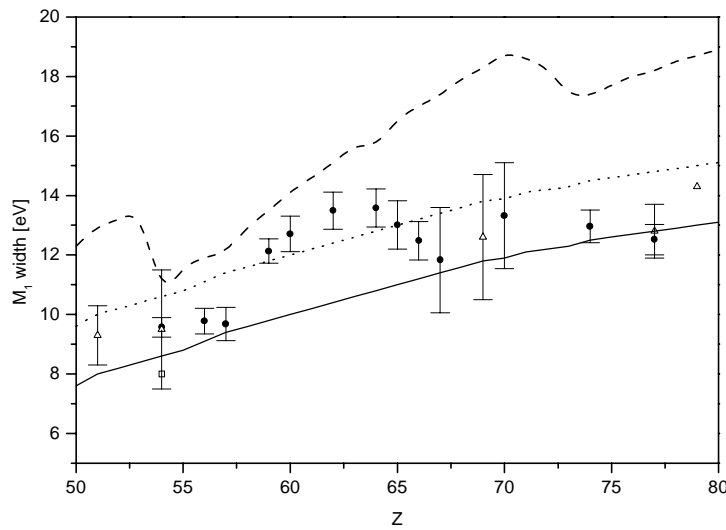


Fig. 3: Width M_1 versus atomic number Z . Present results are depicted by full circles and their variation with Z outside of the lanthanide region by the solid line. The dotted line represents the recommended values of Campbell and Papp [1], the dashed one predictions from the IPM model [6]. Results for ${}_{70}\text{Yb}$, ${}_{74}\text{W}$ and ${}_{77}\text{Ir}$ were obtained previously at the beam-line BM 5. Open symbols stand for experimental data from other sources.

Results are presented graphically in Fig. 3 where they are compared to predictions from the independent particle model (IPM) [6] and the values recommended by Campbell and Papp [1]. The solid line corresponds to a least-squares-fit to our results, lanthanide results excluded. One sees that Campbell and Papp values overestimate present results by about 2 eV. The deviations between the theoretical IPM predictions and our results are even larger. In addition, the resonance-like bump observed in the lanthanide region which is due to the above-mentioned splitting of the M_1 level does not occur in Campbell and Papp's plot, nor in the curve corresponding to the theoretical predictions. Our results will be submitted for publication in Phys. Rev. A. The corresponding paper is in preparation.

References

- [1] J.L. Campbell and T. Papp, At. Data Nucl. Data Tables **77**, 1 (2001).
- [2] T. Papp, J.L. Campbell, J.A. Maxwell, J.-X. Wang and W.J. Teesdale, Phys. Rev. A **45**, 1711 (1992).
- [3] P.-A. Raboud, M. Berset, J.-Cl. Dousse and Y.-P. Maillard, Phys. Rev. A **65**, 022512 (2002).
- [4] J. Hozowska, J.-Cl. Dousse, J. Kern and Ch. Rhême, Nucl. Instr. Meth. Phys. Res. A **376**, 129 (1996).
- [5] J.A. Bearden, Rev. Mod. Phys. **39**, 78 (1967).
- [6] S.T. Perkins et al., LLNL Report No. UCRL-50400, 1991 (unpublished).